MJFAS
Malaysian Journal of Fundamental and Applied Sciences

Minardi *et al.* | Malaysian Journal of Fundamental and Applied Sciences, Vol. 21 (2025) 2394–2405

RESEARCH ARTICLE

The Use of Poisson's Ratio and HVSR Analysis for Clustering Liquefaction Hazard Potential (Case Study: Mandalika Special Economic Zone Buffer Zone)

Suhayat Minardi[a,b]*, Kosim[a], Teti Zubaedah[a], Muhajirah[a], Agustya Adi Martha[c], Muhammad Haikal Havidz[d]

[a]Master's Program in Disaster Mitigation, Postgraduate Program, University of Mataram, Jalan Pendidikan No. 37 Mataram, Indonesia; [b]Physics Study Program, Faculty of Mathematics and Natural Sciences, University of Mataram Jalan Majapahit No. 62 Mataram, Indonesia; [c]Center for Limnology and Water Resources Research, National Research, and Innovation Agency (BRIN), Jl. Raya Jakarta-Bogor No.32, Pakansari, Cibinong, Bogor, Indonesia; [d] Students of the MMB Study Program, Postgraduate Program, University of Mataram, Jalan Pendidikan No. 37 Mataram, Indonesia

Abstract Liquefaction is a geotechnical phenomenon resulting from decreased strength and stability of water-saturated soil due to vibrations or dynamic loads caused by earthquakes. This phenomenon can potentially cause substantial damage to infrastructure and buildings and threaten the safety of humans. The area has never experienced liquefaction, but the Mandalika is a special economic zone (SEZ) that faces directly onto the earthquake source Megatrust of the Indian Ocean, which has the potential to cause an earthquake of 9.0 Mw. The surrounding villages, namely Kuta, Mertak, Sukadana, and Sengkol, support this area. The rapid development of this area as a tourism and infrastructure destination has resulted in the need to understand and mitigate the risk of liquefaction that could impact the safety and sustainability of development in the area. This study aims to cluster the liquefaction potential of the Madalika area and its surroundings based on Poisson's ratio data supported by the results of horizontal to vertical spectrum ratio (HVSR) analysis and groundwater depth data. Microseismic data were measured at around 60 points spread throughout the research area. Poisson's ratio was calculated from the primary and secondary wave velocities of ground profiling microseismic data and groundwater level data measured in dug wells owned by residents. The value of the Poisson's ratio in the study area is about 0.1 to 0.5. Observing high or low Poisson's ratio values can help determine the potential for liquefaction moments caused by vibration and estimate the level of liquefaction risk in the Mandalika area. Poisson's ratio data was supported with data on sediment thickness, about (4 – 129) meters, (1 – 5) meters of groundwater level, and (64 – 918) ms^{-1} of V_{s-30} to determine class potential liquefaction. The ranking or class liquefaction is based on factors influencing a row occupied by Kuta Village, Sengkol Village, Sukadana Village, and Mertak Village.

Keywords: Class potential, HVSR, liquefaction, buffer village of Mandalika, influential factors.

***For correspondence:**
suhayat.minardi@unram.ac.id

Received: 24 April 2025
Accepted: 15 July 2025

Introduction

Mandalika Special Economic Zone (SEZ) is an area developed for tourism with draft ecotourism sustainability [1]. Located in the southern part of Lombok Island, which faces directly onto the Indian Ocean, there is a subduction zone between the Indo-Australian and Euro-Asian Plate[2]. Some geophysical research in the Mandalika Special Economic Zone includes seawater intrusion[3], [4], aquifers [5], and thickness of the sediment [6].

Geologically, the Mandalika area was formed by Quaternary alluvial deposits, consisting of rough sand, fine sand, shale, clay, and many places found in fraction animal sea [7]. Areas with characteristics such

as Mandalika, directly adjacent to the coastline, composed of alluvial sediment layers and shallow groundwater levels, can experience liquefaction if shaken by an earthquake of more than 7.0 Mw. These characteristics are similar to those of the Lolu village, Jono Oge District Sigi experienced liquefaction during the 2018 Palu Donggala Earthquake [8]**.** Although there are no records of liquefaction events in the area, the position of Mandalika and its surroundings is directly opposite the subduction zone, the source zone of the Megathrust earthquake, which has the potential to generate a 9.0 Mw earthquake [9].

Apart from earthquakes, geological factors can increase the risk of liquefaction. Reference [10] stated that several factors that influence liquefaction potential are rock age and groundwater depth, as shown in Table 1.

Table 1. A map of liquefaction susceptibility's production considerations in the San Fernando Valley

Age of Deposit	Depth of Groundwater (feet)		
	D < 10	10 ≤ D < 30	D ≥ 30
Latest Holocene	High	Low	Nil
Earlier Holocene	Moderate	Low	Nil
Late Pleistocene	Low	Nil	Nil

According to other sources, liquefaction transforms water-saturated sandy soil into liquid because dynamic pressures like cyclic earthquake loads raise the pore water pressure. Liquefaction usually occurs in water-saturated soil, where all cavities are filled with water [11]. The type of soil most at risk of liquefaction is non-cohesive, in this case, sand. The risk will be greater if the grain size is smaller or finer [12].

Liquefaction is the loss of strength and stiffness in water-saturated soil, frequently brought on by earthquakes or other vibrations. Reference [13] states that liquefaction may occur in areas composed of locally deposited sediments such as sand, loose soil, or silt, particularly when these materials exhibit water-saturated, low-density, granular characteristics, as shown in Figure 1. Such soils are typically non-cohesive, contain elevated pore water pressure within the sediment matrix, and are associated with a shallow groundwater level. The potential will be more significant if the area has potential movement surface seismic over threshold value due to the instant existence of vibration land, a consequence of earthquake earth. Furthermore, the risk of liquefaction increases during earthquakes of prolonged duration or repeated seismic events [14].

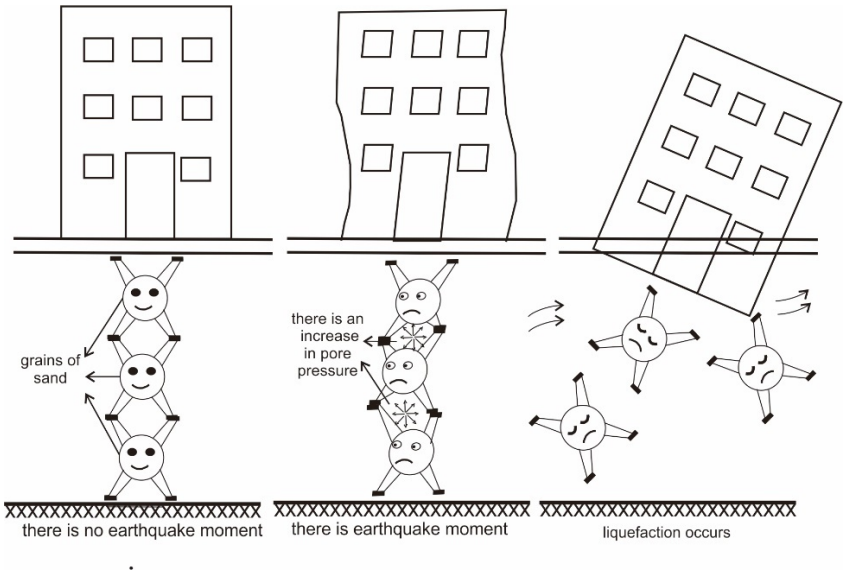

Figure 1. Sediment behavior during liquefaction

Poisson's ratio is a key parameter used to evaluate the physical quality of rocks. Its value varies depending on the degree of deformation [15] and is related to rock quality [16], as shown in equation 1.

$$v_{rm} = 0.25(1 + e^{-0.2\sigma_{rm}}) \quad (1)$$

with v_{rm} is the Poisson's ratio of the rock mass and σ_{rm} is the strength of the rock mass.

In geological contexts, Poisson's ratio is associated with pore fluid saturation [17] and is influenced by hydrostatic pressure within the rock mass[18]. In addition, the Poisson's ratio value is also related to sandstone elasticity [19], the pressure and geological strength index [20], the geomechanical behavior of sedimentary rocks with elastic wave velocity [21], Poisson's ratio in hard rocks [22], and Poisson's ratio in shallow sediments and topsoil [23]. From various studies, it can be seen that the Poisson's ratio value can indicate the quality of a rock.

Poisson's ratio (υ) is the ratio of transverse strain (or lateral contraction) to longitudinal strain resulting from normal stress changes due to compression or expansion. It can be determined dynamically using the velocities of compressional (Vp) and shear (Vs) waves in rock, typically obtained from seismic data or sonic logging. This dynamic calculation method is commonly used in geophysical studies, as expressed in Equation (2) [24].

$$\upsilon = \frac{\left(\frac{v_p}{v_s}\right)^2 - 2}{2\left[\left(\frac{v_p}{v_s}\right)^2 - 1\right]} \quad (2)$$

Vp is the compressional (P-wave) velocity value, and Vs is the shear (S-wave) values. The relationship between the ratio Vp / Vs and ν is shown in Figure 2. For a typical value of ν = 0.25 for rock, Vp/Vs = 2.24 [25].

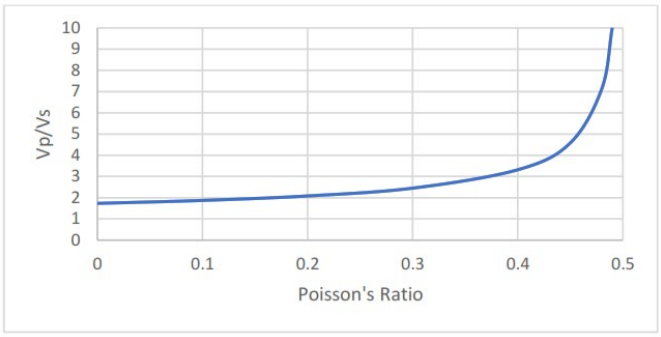

Figure 2. Poisson's ratio as a function of Vp/Vs[25]

Poisson's ratio can serve as an indicator of water content (soil moisture) in the ground. Changes in soil moisture can significantly affect soil elasticity, Poisson's ratio, and overall geo-mechanical behavior [26]. The relationship between rock type and corresponding Poisson's ratio values is presented in Table 2.

Table 2. Poisson's ratio values of various types of rocks [27]

Type of Soil	Poisson's Ratio (μ)
Clay, saturated	0.4 – 0.5
Clay, unsaturated	0.1 – 0.3
Sandy clay	0.2 – 0.3
Silt	0.3 – 0.35
Sand, gravelly sand	-0.1 – 1.00
commonly used	0.3 – 0.4
Rock	0.1 – 0.4 (dependent somewhat on the type of rock)
Loess	0.1 – 0.3
Ice	0.36
Concrete	0.15
Steel	0.33

According to the influence of degrees saturation on the mark ratio of Poisson land, from the depiction mentioned, it is seen that degrees saturation significantly affects Poisson's ratio.

Previous research on liquefaction potential using Poisson's ratio was conducted by [28] where velocity data were obtained through Multichannel Analysis of Surface Waves (MASW). In that study, liquefaction analysis was based solely on rock groundwater saturation, which is directly related to Poisson's ratio. HVSR and MASW methods are two seismic methods used for ground profiling. Each method has advantages and disadvantages in terms of methodology, depth range, and inversion results. The HVSR inversion result is in the form of HVSR curve fitting, while the MASW method produces a dispersion curve. Combining both methods increases the accuracy of the shear wave velocity profile, which is important for seismic hazard assessment [29].

In contrast, the present study evaluates liquefaction potential using Poisson's ratio and other influencing factors, including **soil type**, **groundwater level**, and sediment **thickness**. All input data, except groundwater level, were derived from microtremor analysis. Microtremors are natural ground vibrations with amplitudes ranging from 0.1 to 1.0 microns and velocities between 0.001 and 0.010 cm·s^{-1}[30].

HVSR analyzes the spectrum of Rayleigh waves propagating in the sediment layers above bedrock, which is relatively more rigid than sediment rock. The influence of Rayleigh waves on the recording signal microtremor has the same value for vertical and horizontal components when the range frequency is 0.2 Hz to 20 Hz. Calculation of spectrum ratio of microtremor vertical component to horizontal component (HVSR) using Equation 3

$$HVSR = \frac{S_{HS}}{S_{VS}} = \frac{\sqrt{[(S_{North-South})^2 + ((S_{West-East})^2]}}{S_{Vertikal}} \quad (3)$$

An analysis of HVSR is applied to microtremor data to extract key parameters related to three factors influencing liquefaction: soil type, sediment thickness, and shear wave characteristics. The HVSR analysis yields two main outputs: **natural frequency** and **amplification factor,** as shown in Figure 3.

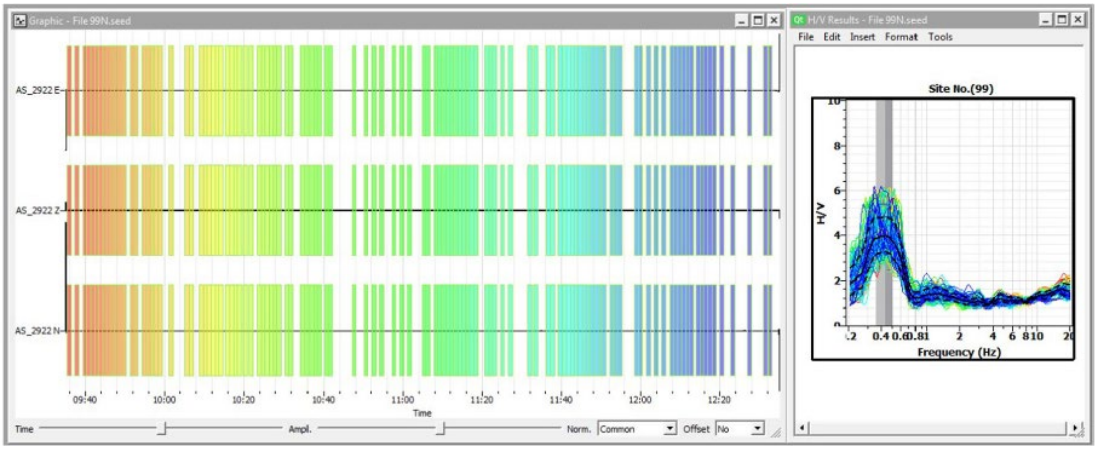

Figure 3. Results of microseismic data processing with HVSR [31]

The HVSR method generates microtremor spectra with a prominent peak at the predominant frequency. The key parameters derived from this analysis are the **dominant frequency (f_0),** is directly proportional to the average shear wave velocity (Vs) and inversely proportional to the thickness of the surface sediments [32]. The **amplification factor (A_0)**, which provide insight into the dynamic characteristics and subsurface soil layers. The resonance phenomenon in sedimentary layers is the trapping of seismic waves in the surface layer due to the impedance contrast between the sedimentary layer and deeper hard rocks. Interference between seismic waves trapped in the sedimentary layer develops into a resonance pattern related to the sedimentary layer's characteristics[33], as shown in Figure 4.

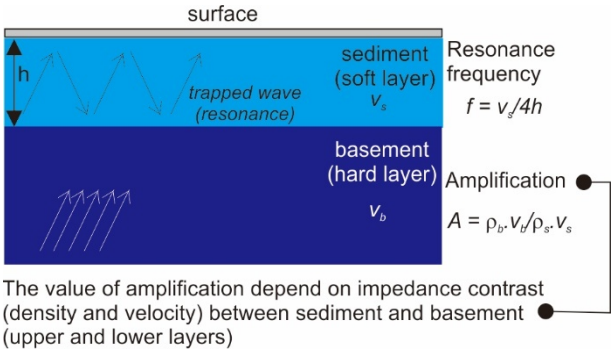

Figure 4. The existence of trapped waves which produce an amplification (A)

The HVSR theory states that there is a correlation between sediment thickness and liquefaction risk, as formulated in equation 4.

$$K_g = \frac{4.A_0^2.d}{v_s} \tag{4}$$

K_g is the earthquake vulnerability, A_0 is the amplification factor, d is the sediment thickness, and v_s is the secondary wave velocity. The Equation shows that the earthquake vulnerability value is directly proportional to the sediment thickness [34].

To estimate the **shear wave velocity (Vs)** and **primary wave velocity (Vp)**, the HVSR curve is inverted using a **Monte Carlo algorithm**, enabling subsurface structure modeling beneath the microtremor measurement point. Inversion is based on the neighborhood algorithm [35] to find the minimum misfit, as shown in equation 5.

$$misfit = \sqrt{\frac{1}{N}\cdot\sum_{i=1}^{N}\left(\frac{D_i - M_i}{\sigma_i}\right)^2} \tag{5}$$

where N is the number of data, D_i, M_i, and σ_i are, respectively, the inversion results, soil structure model, and standard deviation of the inversion data. The misfit value used to determine the best model is the lowest in the 0 to less than one range. If the misfit value is still high (more than 1), changes must be made to the initial model parameters [36].

Following this, **data fitting** is performed to match observed and theoretical curves. The accuracy of this fitting is evaluated using the **misfit (error value)**. The result of the HVSR curve inversion is presented as a velocity profile, as shown in **Figure 5**.

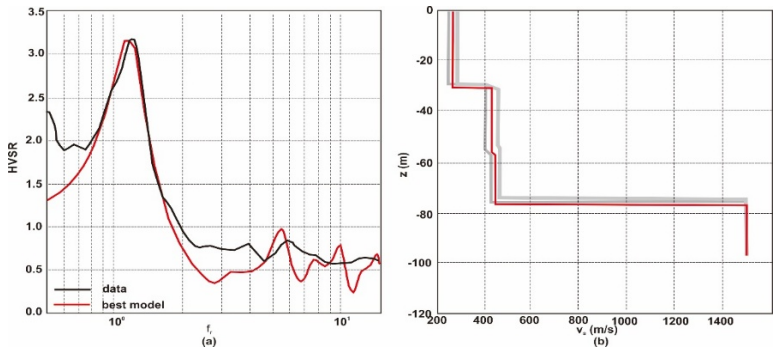

Figure 5. (a) Comparison of the HVSR curve from field measurements with the best model of HVSR inversion; (b) Model 1-D Shear wave velocity (Vs)[36]

One factor influencing liquefaction is the velocity of the shear wave (v_s) in matter. The average wave shear wave velocity (v_s) was used up to a thickness of 30 m (v_{s-30}). The calculation of v_{s-30} is carried out by using the result data inversion HVSR curve and Equation 6 [37]

$$v_{s-30} = \frac{30}{\sum_1^m \frac{h_i}{v_i}} \tag{6}$$

with i as the layering index, m is the number of layers (in this study, analyzed up to a depth of 30 meters), h_i It is the thickness of the i-th layer v_s. the velocity of the shear wave. The velocity value of the shear wave (v_{s-30}) can be used as a base for pressing the vulnerability of a layer to dangerous liquefaction, such as in Table 3

Table 3. Value of v_{s-30} based on SNI 1726:2019[37]

Class	*Vs.- 30* value (m/s)	Description
SA	≥1500	Hard soil, **not prone** to liquefaction
SB	750 ≤Vs. ≤1500	Medium soil, **susceptible** to liquefaction
SC	350 ≤Vs. ≤750	Soft soil, **very vulnerable** to liquefaction
SD	175 ≤Vs. ≤350	Soft soil, **very vulnerable** to liquefaction and collapsed land
SE	≤ 175	Soft soil, **very vulnerable** to liquefaction, landslide, and damaged building

The table above shows layers with the $V_{s.-30}$ less from 1500 m/s vulnerable to danger liquefaction. Because of shock, the consequence of earthquakes is more decisive on the layer with speed waves with low shear.

The sediment thickness has no relation to factor amplification. However, the thickness of sediment can enlarge, strengthening earthquake waves. On the other hand, the area with high amplification predicted its characteristics, such as soft rock and thick, high sediment. That causes trapped wave earthquakes in sediments, making the area vulnerable to multi-reflection waves. The resonance frequency can be utilized to determine the depth of the soft sediments within the study region where changes in S-wave velocity are minimal. The relation between sediment depth and resonance frequency was presented in Equation 7 [38].

$$f_0 = \frac{v_s}{4h} \quad \text{or} \quad h = \frac{v_s}{4f_0} \tag{7}$$

The sediment thickness influences how easily land can experience liquefaction, depending on how sediment interacts with other factors such as compaction, humidity, and intensity vibration. More sediment thickness values can increase the risk of liquefaction if other conditions support the occurrence.

Materials and Methods

Microseismic data was measured in the Mandalika area at 60 points spread across the region. Groundwater level data was measured at dug wells owned by residents around the microseismic measurement points. Microseismic measurement was used for the seismometer SRI, as presented in Figure 6.

Figure 6. Seismometer SRI and measuring micro-seismic using SRI [39]

Data have been processed using the HVSR (Horizontal to Vertical Spectral Ratio) method. Stages of data processing are displayed in Figure 7.

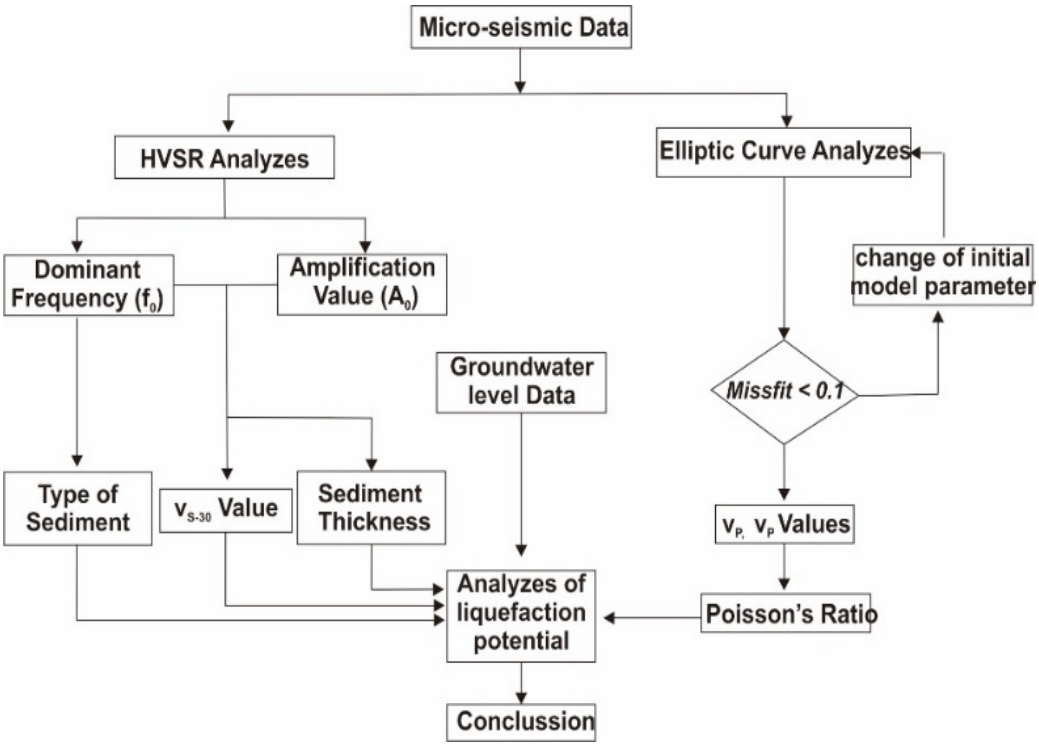

Figure 7. Stages study analyst potential liquefaction based on microtremor data.

Device software used in this data processor is Geopsy and Dinver, which are used for HVSR analysis and inversion HVSR curve, Microsoft Excel for count parameters of micro-seismic, QGIS for plotting the result processing data, and Corel Draw for editing picture map.

Results and Discussion

The average velocity of shear waves with a depth of 30 meters (v_{s-30}) is an essential parameter in ground movement analysis. Layers with a low of v_s value have low stiffness value, so the earthquake that passes through it will experience strengthening or more amplification compared to hard soil. The distribution of v_{s-30} values of the study area is presented in Figure 8.

The v_{s-30} value in the study area ranges from 64 ms^{-1} to 918 ms^{-1}. Based on Table 2, the soil/rock in the study area is categorized as soft to medium soil. With these conditions, the study area is vulnerable to liquefaction potential in the vulnerable to very vulnerable category.

Based on the soil type, the research area is dominated by alluvial deposits. Rocks or soil on the surface are in the form of loose sand. So, based on [12] the research area has the liquefaction potential, and non-cohesive sand layers are layers that are easily filled with water, which easily lose their strength if they experience shocks due to earthquakes.

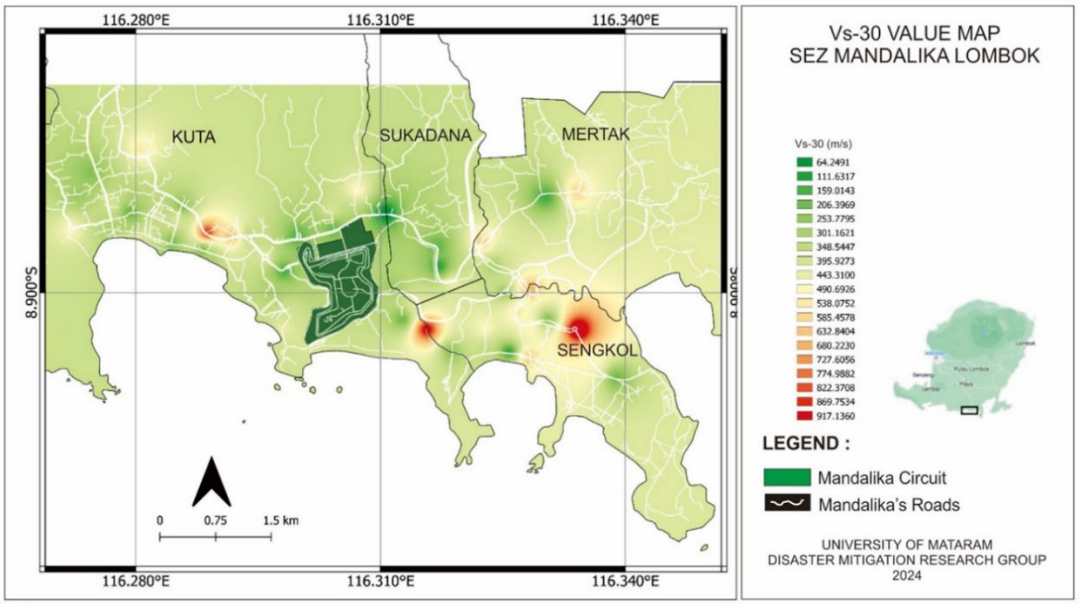

Figure 8. Distribution of v_{s-30} value

The thickness of the sediment layer significantly influences the amplification of seismic waves during an earthquake. In areas with the same rock properties, sediment layers less than 10 meters thick tend to produce lower amplification than areas with thicker sediment deposits. Thicker sediment layers can induce **resonance effects**, enhancing seismic wave amplitude. The depth estimation results, calculated using Equation 3**,** are shown in Figure 9**.**

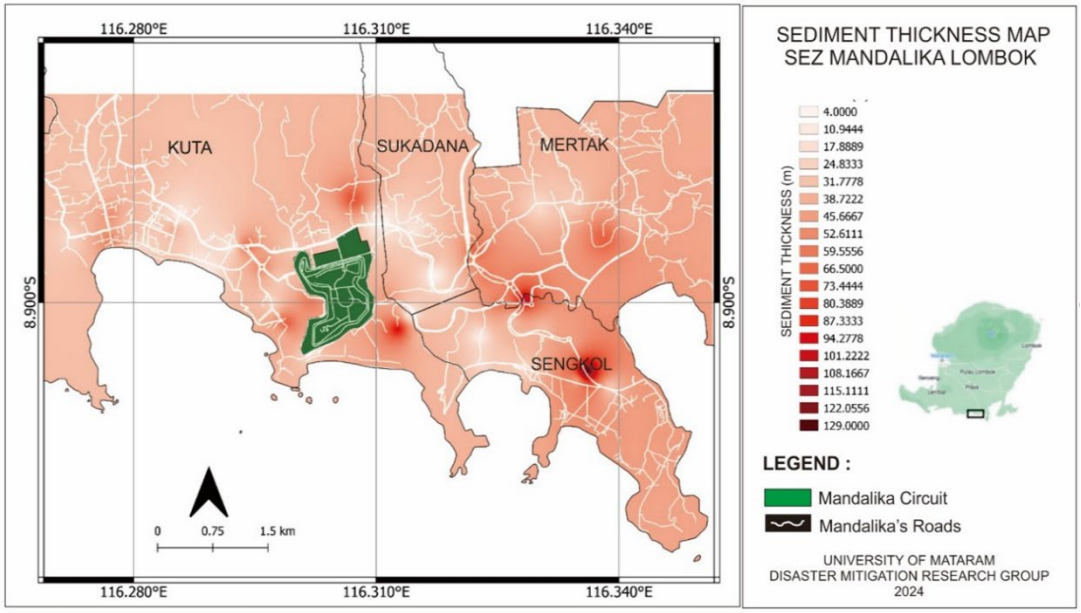

Figure 9. Distribution map of sediment thickness

Sediment thickness plays a critical role in the amplification of seismic waves. Greater amplification results in stronger ground shaking, which increases the susceptibility of soil and rock bodies to liquefaction. Based on this relationship, **Sengkol, and Kuta villages** are identified as having the highest liquefaction potential within the study area due to their relatively thick sediment layers.

Sediment thickness plays a critical role in the amplification of seismic waves. Greater amplification results in stronger ground shaking, which increases the susceptibility of soil and rock bodies to liquefaction. Sediment thickness does not directly affect liquefaction, but based on the HVSR theory of [34], sediment thickness is directly proportional to earthquake vulnerability and amplification factor value. All of these will accelerate the loss of soil strength when an earthquake occurs. In other words, based on Figure 9, the thickness of the sediment in the research area reaches 129 meters. The thicker the sediment, the more devastating the impact of the earthquake. The direct impact is in the form of large amplification; the damage is getting worse due to the higher level of vulnerability, and the process of losing soil strength will be faster and easier. Based on this relationship, **Sengkol, and Kuta villages** are identified as having the highest liquefaction potential within the study area due to their relatively thick sediment layers.

Liquefaction typically occurs in **unconsolidated sandy soils** that are saturated with water. The liquefaction potential is generally found at groundwater depths less than 15 meters, with the highest risk occurring when groundwater is less than 3 meters. The vulnerability decreases at groundwater depths between 3 and 9 meters and is lowest when the groundwater level exceeds 9 meters.

The spatial distribution of groundwater depth in the study area is shown in Figure 10.

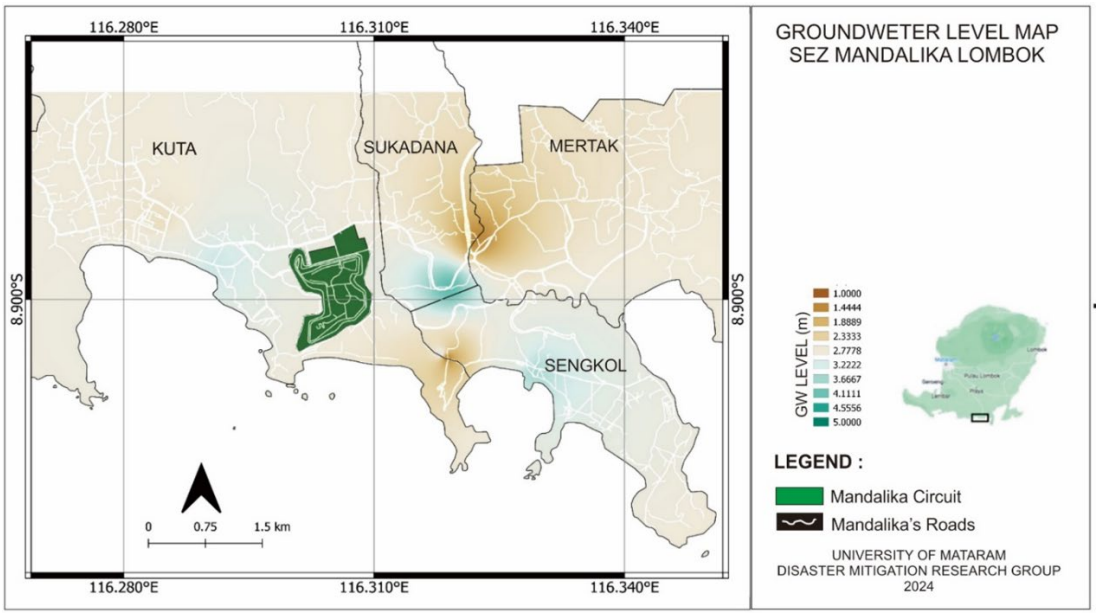

Figure 10. Distribution depth groundwater level

During an earthquake, **liquefaction may result in water and sand/mud ejection**—often in surface eruption or ground deformation—in areas with shallow groundwater levels. This phenomenon reduces or eliminates the cohesion between soil particles, significantly diminishing the soil's bearing capacity and increasing the likelihood of structural damage.

Poisson's ratio can be derived from elastic wave velocities, specifically the **compressional wave velocity (Vp)** and the **shear wave velocity (Vs)**. The value of Poisson's ratio is calculated using Equation 2.

Poisson's ratio is valuable for distinguishing between **consolidated and unconsolidated** rock types. Consolidated rocks generally exhibit lower Poisson's ratio values, while **unconsolidated or porous rocks** tend to have higher values.

Poisson's ratio value is a quantity that describes all conditions. Table 2 shows that the value is related to water saturation, where the higher the water saturation, the higher the Poisson's ratio value, or saturation is directly proportional to the Poisson's ratio value. Soft rocks, in this case non-cohesive sand, can store water more than other rocks in the research area. The higher the groundwater level, the larger the rock column filled with water or the relatively greater saturation. The Poisson's ratio value is greater if the

saturation is greater. The spatial distribution of Poisson's ratio values within the study area is shown in Figure 11.

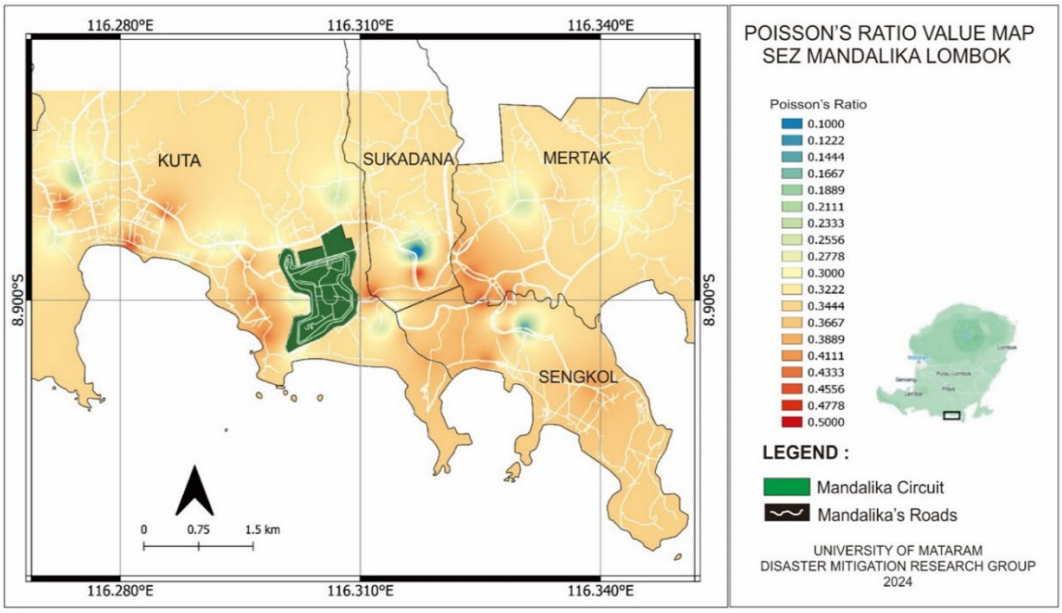

Figure 11. Distribution of Poisson's ratio values

Based on Figure 11, the Poisson's ratio value of the research area ranges from 0.1000 to 0.4778. Areas bordering the coastline have low Poisson's ratio values, namely Kuta Village and Sengkol Village. The low value of Poisson's ratio is often considered an indicator of risk liquefaction. However, the high value of Poisson's ratio is also susceptible to liquefaction in some cases, especially for unconsolidated materials like soil and sediment. From the distribution of Poisson's ratio values, the areas with the most significant potential for liquefaction are Kuta Village, Sengkol Village, Pujut Village, and Sukadana Village.

The potential level of liquefaction, in a simple way, is determined based on the class/rank of the factors that influence liquefaction, namely thickness sediment, height groundwater level, and Poisson's ratio. These three factors have the same weight in determining potential liquefaction. The lowest value of one of these three factors in one place shows the factors in the area with the amount marked lowest means the parameters obtained from measurements in the area study that are mark $v_{s\text{-}30}$, thickness sediment, groundwater level, and Poisson's ratio. Measurement results classified with method share become three value level classification results measuring high, medium, and low levels, where these levels are only for area research and are not applicable in general.

In simple terms, the order of liquefaction potential levels, when viewed from the four factors that influence liquefaction, is shown in Table 4.

Table 4. Rank of potential due to factors trigger liquefaction

	Kuta	Mertak	Sukadana	Sengkol
Poisson's ratio	1	4	3	2
Average velocity up to 30 m depth	1	4	2	3
Height of groundwater level	1	3	4	2
Thickness Sediment	2	4	3	1
Amount	5	14	12	8
Rank of potential liquefaction	**1**	**4**	**3**	**2**

Poisson's ratio value can be used as a basis for seeing the liquefaction potential of an area. Based on Table 4 above, the liquefaction potential class based on Poisson's ratio value is supported by other factors, such as the $v_{s\text{-}30}$ value, groundwater level, and sediment thickness. From this table, it can be seen that Kuta Village has the highest potential based on three factors that affect liquefaction. Meanwhile, Sengkol Village only has the liquefaction potential based on the thickness of its sediment.

In addition to being displayed in tabular form, the ranking of liquefaction potential is also displayed as an overlay of contour maps of the four factors, as shown in Figure 12. Contours with small closure shapes indicate extreme values of each factor.

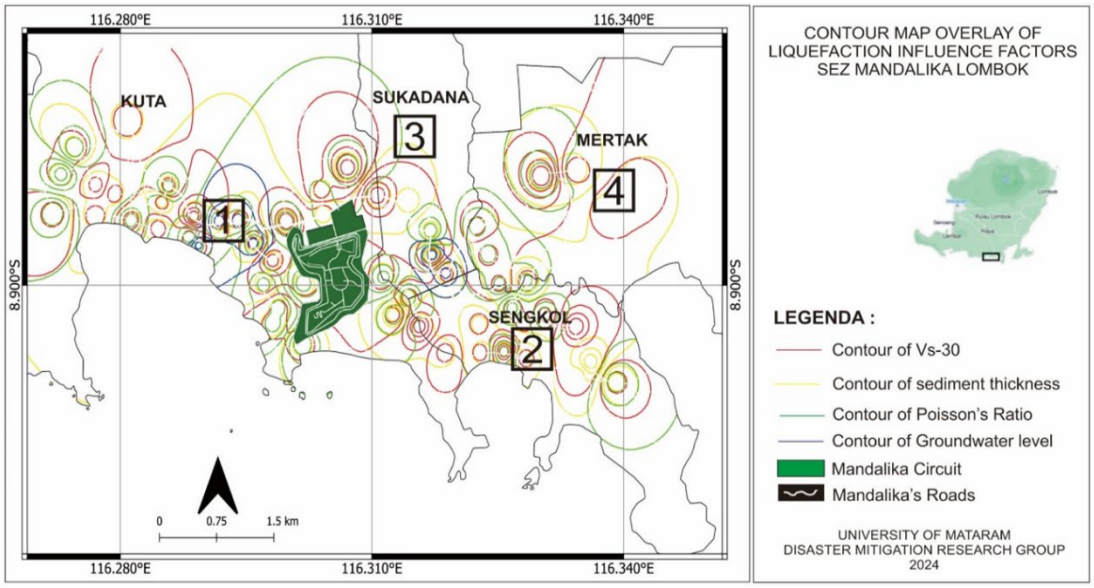

Figure 12. Contour overlay thickness sediment, depth groundwater level, and value Poisson's ratio and risk level ranking liquefaction

Conclusions

Based on the above analysis, Poisson's ratio can indicate liquefaction potential, particularly in coastal areas. The liquefaction potential was assessed by evaluating several influencing factors, resulting in the following ranking: **Kuta Village** has the highest liquefaction potential, followed by **Sengkol Village**, **Sukadana Village**, and **Mertak Village**, which has the lowest potential for liquefaction.

Conflicts of Interest

The authors declare that there is no conflict of interest regarding the publication of this paper.

Acknowledgements

Thanks to the University of Mataram for funding this research through the Postgraduate Research scheme with Contract No. 1643/UN18. L1/PP/2024.

References

[1] Estriani, H. N. (2019). *Prodi Ilmu Hubungan Internasional FISIP UPN "Veteran" Jakarta Kawasan Ekonomi Khusus (KEK) Mandalika dalam implementasi konsep pariwisata berbasis ecotourism: Peluang dan tantangan*.

[2] Maharani, Y. N., Septiadhi, A., & Algary, T. A. (2022). Pemetaan jalur evakuasi sebagai upaya pengurangan risiko bahaya tsunami di wilayah Kuta Mandalika, Provinsi Nusa Tenggara Barat, Indonesia.

[3] Alaydrus, A. T., Susilo, A., Naba, A., & Minardi, S. (2021). Identification of the constraints of physical properties on fluid flow rate (as a preliminary study for analysis of changes in subsurface conditions in the KEK Mandalika Lombok). *Journal of Physics: Conference Series, 1816*(1), 012100. https://doi.org/10.1088/1742-6596/1816/1/012100

[4] Alaydrus, A. T., Susilo, A., Naba, A., Minardi, S., & Azhari, A. P. (2024). Investigation of seawater intrusion in Mandalika, Lombok, Indonesia using time-lapse geoelectrical resistivity survey. *International Journal of Design and Nature and Ecodynamics, 19*(1), 1–11. https://doi.org/10.18280/ijdne.190101

[5] Alaydrus, A. T., Susilo, A., Minardi, S., Naba, A., & Abraham, T. P. (2023). 3D inversion modelling of gravity and geomagnetic in the coastal aquifer of the Mandalika Lombok. *IOP Conference Series: Earth and Environmental Science, 1175*(1), 012018. https://doi.org/10.1088/1755-1315/1175/1/012018

[6] Minardi, S., Ardianto, T., Alaydrus, A. T., Tawakal, M. I., & Martha, A. A. (2023). Investigation of sediment thickness

beneath the Mandalika circuit and its surroundings based on microtremor data. *International Journal of GEOMATE, 25*(112), 40–47. https://doi.org/10.21660/2023.112.4108

[7] Wafid, M., Sugianto, Tulus, P., & Sarwondo. (2014). *Resume hasil kegiatan pemetaan geologi teknik Pulau Lombok skala 1:250.000*.

[8] Agustian, Y. (2021). Likuefaksi. *Jurnal Ilmiah Teknologi Informasi Terapan, 8*(1), 209–215. https://doi.org/10.33197/jitter.vol8.iss1.2021.749

[9] Irsyam, M., *et al.* (2015). Development of seismic risk microzonation maps of Jakarta city. In *Geotechnics for catastrophic flooding events* (pp. 35–47). Taylor and Francis. https://doi.org/10.1201/b17438-6

[10] Housner, G. W. (1985). *Liquefaction of soils during earthquakes*.

[11] Musa Sjahrain, U., Rondonuwu, S. G., & Riogilang, H. (2021). Analisis potensi likuifaksi dengan menggunakan parameter kuat geser tanah lempung.

[12] Deo, P., Prayitno, & Artati, H. K. (2021). Analisis potensi likuifaksi berdasarkan distribusi ukuran butir tanah dan data cone penetration test (CPT).

[13] Seed, B. H., & Idriss, I. M. (1970). *National Technical Information Service: A simplified procedure for evaluating soil liquefaction potential*.

[14] Day, R. W. (2002). *Geotechnical earthquake engineering handbook*. McGraw-Hill.

[15] Dong, L., Xu, H., Fan, P., & Wu, Z. (2021). On the experimental determination of Poisson's ratio for intact rocks and its variation as deformation develops. *Advances in Civil Engineering, 2021*, 8843056. https://doi.org/10.1155/2021/8843056

[16] Narimani, S., Davarpanah, S. M., & Vásárhelyi, B. (2024). Estimation of the Poisson's ratio of the rock mass. Budapest University of Technology and Economics. https://doi.org/10.3311/PPci.22689

[17] Raharjo, W., Palupi, I. R., Nurdian, S. W., Giamboro, W. S., & Soesilo, J. (2016). Poisson's ratio analysis (Vp/Vs) on volcanoes and geothermal potential areas in Central Java using tomography travel time method of grid search relocation hypocenter. *Journal of Physics: Conference Series, 776*(1), 012114. https://doi.org/10.1088/1742-6596/776/1/012114

[18] Wang, Q., & Ji, S. (2009). Poisson's ratios of crystalline rocks as a function of hydrostatic confining pressure. *Journal of Geophysical Research: Solid Earth, 114*(9). https://doi.org/10.1029/2008JB006167

[19] Arns, C. H., Knackstedt, M. A., & Pinczewski, W. V. (2002). Accurate Vp:Vs relationship for dry consolidated sandstones. *Geophysical Research Letters, 29*(8). https://doi.org/10.1029/2001GL013788

[20] Lógó, B. A., & Vásárhelyi, B. (2020). Parametric study on the connection between Poisson's Ratio, GSI and environmental stress. *Computer Assisted Methods in Engineering and Science, 27*(2–3), 205–217. https://doi.org/10.24423/cames.287

[21] Garia, S., Pal, A. K., Nair, A. M., & Ravi, K. (2020). Elastic wave velocities as indicators of lithology-based geomechanical behaviour of sedimentary rocks: An overview. Springer Nature. https://doi.org/10.1007/s42452-020-03300-1

[22] Bukowska, M., Kasza, P., Moska, R., & Jureczka, J. (2022). The Young's modulus and Poisson's ratio of hard coals in laboratory tests. *Energies, 15*(7). https://doi.org/10.3390/en15072477

[23] Essien, U. E., Akankpo, A. O., & Igboekwe, M. U. (2014). Poisson's ratio of surface soils and shallow sediments determined from seismic compressional and shear wave velocities. *International Journal of Geosciences, 5*(12), 1540–1546. https://doi.org/10.4236/ijg.2014.512125

[24] Zhang, J. J., & Bentley, L. R. (2005). Factors determining Poisson's ratio.

[25] Poulos, H. G. (2021). Use of shear wave velocity for foundation design. https://doi.org/10.21203/rs.3.rs-493427/v1

[26] Yan, K., Wang, Y., Lai, X., Wang, Y., & Yang, Z. (2023). Experimental study on Poisson's ratio of silty-fine sand with saturation. *Journal of Marine Science and Engineering, 11*(2). https://doi.org/10.3390/jmse11020427

[27] Bowles, J. E. (1997). *Foundation analysis and design*. Irwin/McGraw-Hill.

[28] Mandasari, S., Asrillah, & Rusydy, I. (2017). Studi likuifaksi menggunakan nilai Poisson's ratio di Kecamatan Meurah Dua, Pidie Jaya.

[29] Gorstein, M., & Ezersky, M. (2015). Combination of HVSR and MASW methods to obtain shear wave velocity model of subsurface in Israel. *International Journal of Geohazard and Environment, 20–41*.

[30] Mirzaoglu, M., & Dýkmen, Ü. (2003). Application of microtremors to seismic microzoning procedure.

[31] Moustafa, S. S. R., Mohamed, A., Abdelhafiez, H. E., El-Faragawy, K., & Ali, S. (2023). A fusion approach for evaluating ground conditions for seismic microzoning at the Egyptian Solar Park in Benban, Aswan. *Environmental Earth Sciences, 82*(12). https://doi.org/10.1007/s12665-023-10968-2

[32] Nakamura, Y. (1989). Clear identification of fundamental idea of Nakamura's technique and its applications. https://www.researchgate.net/publication/228603691

[33] Hamimu, L. H., Juarzan, L. I., & Pathiasari, N. I. (2023). Analisis ketebalan lapisan sedimen menggunakan metode horizontal to vertical spectral ratio (HVSR) di daerah perbukitan Kecamatan Moramo. *Jurnal Rekayasa Geofisika Indonesia, 6*(01), 1–15. https://doi.org/10.56099/jrgi.v6i01.29

[34] Nakamura, Y. (2008). On the H/V spectrum.

[35] Sambridge, M. (1999). Geophysical inversion with a neighbourhood algorithm – I. Searching a parameter space. *Geophysical Journal International, 138*(2), 479–494. https://doi.org/10.1046/j.1365-246X.1999.00876.x

[36] Sunardi, B., Susilanto, P., & Putri, E. N. (2017). Penerapan metode inversi HVSR untuk pencitraan 3-D kecepatan gelombang geser (Vs) di Kulon Progo bagian selatan. *Jurnal Riset Geofisika Indonesia, 1*(2), 53–59. https://www.researchgate.net/publication/322695502

[37] Badan Standardisasi Nasional. (2012). *Tata cara perencanaan ketahanan gempa untuk struktur bangunan gedung dan non gedung*. www.bsn.go.id

[38] Tian, B., Du, Y., You, Z., & Zhang, R. (2019). Measuring the sediment thickness in urban areas using revised H/V spectral ratio method. *Engineering Geology, 260*. https://doi.org/10.1016/j.enggeo.2019.105223

[39] Semesta. (2024). *SRI seismometer technical specification*.